

Angle-resolved photoemission from Cr(110): Observation of a bulk magnetic phase transition

Y. Sakisaka, T. Komeda, and M. Onchi

Department of Chemistry, Faculty of Science, Kyoto University, Kyoto 606, Japan

H. Kato

Photon Factory, National Laboratory for High Energy Physics, Oho-machi, Ibaraki 305, Japan

S. Suzuki

Department of Physics, Faculty of Science, Tohoku University, Sendai 980, Japan

K. Edamoto

Department of Chemistry, Faculty of Science, Tokyo Institute of Technology, Ookayama, Tokyo 152, Japan

Y. Aiura

Institute of Physics, University of Tsukuba, Sakura-mura, Ibaraki 305, Japan

(Received 2 September 1987; revised manuscript received 4 January 1988)

Normal-emission photoelectron spectra were recorded from Cr(110) at 80 K (below the Néel temperature of $T_N = 312$ K) with photon energies from 20 to 120 eV. Assuming a free-electron final band, bulk energy-band dispersions along the [110] (ΓM) direction normal to the surface are determined. The results are compared with previously calculated band structures for the antiferromagnetic phase. Contrary to earlier claims, we find no evidence for a valence-band satellite in Cr. Temperature-dependent studies were also presented that reveal the disappearance of an emission from the Σ_3 initial-state band (corresponding to the G_3 band in the paramagnetic phase) at temperatures above T_N for a specific \mathbf{k} region. This result is discussed in terms of the bulk magnetic phase transition.

I. INTRODUCTION

The band structure of Cr has been a subject of high interest for experimental¹⁻⁵ and theoretical studies,⁶⁻¹³ since metallic Cr is one of the few known examples of an itinerant antiferromagnet. Bulk Cr crystallizes in a body-centered-cubic (bcc) structure and has an antiferromagnetic (AF) spin arrangement below the Néel temperature of $T_N = 312$ K. In a simple AF structure, atoms in the body-centered positions of the bcc lattice have spins pointing only in one direction and atoms in the corner positions have spins in the opposite direction [see Fig. 1(a)]. Thus this AF Cr has a crystallographic bcc lattice but a magnetic simple-cubic (sc) lattice (CsCl type). However, the true AF ground state is modulated by a spin-density wave (SDW),^{14,15} which is incommensurate with the lattice period. This SDW is sinusoidal and runs along one of the $\langle 100 \rangle$ directions with a wavelength of approximately 21 lattice spacings [i.e., the so-called nesting wave vector \mathbf{Q} is $(2\pi/a)(1 \pm \delta, 0, 0)$, where a is the lattice constant of 2.884 Å and δ is typically 0.048–0.049].

The band-structure calculation for the true incommensurate ($\delta \neq 0$) AF SDW ground state of bulk Cr is not possible. A great number of band-structure calculations were performed for the paramagnetic (PM) phase.^{6-11,13} For the commensurate ($\delta = 0$) AF phase, several calculations have been reported,^{6,10,12,13} where the slight departure of the \mathbf{Q} vector from $2\pi/a$ is ignored. Such an ap-

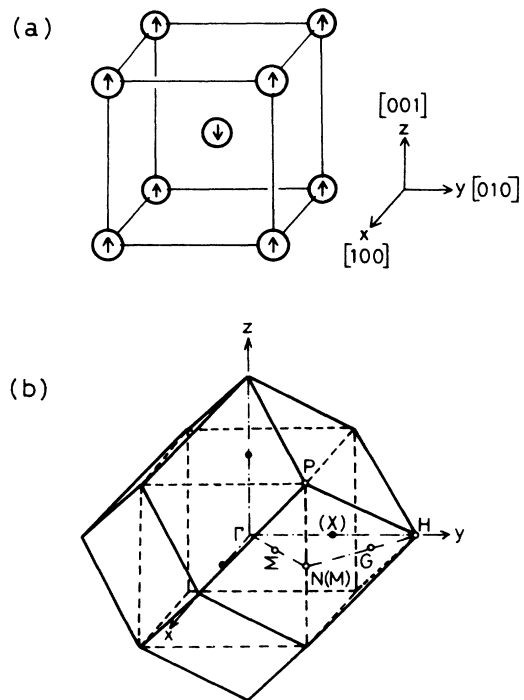


FIG. 1. (a) CsCl structure as magnetic unit cell for commensurate AF Cr. (b) The relation between bcc (solid lines) and sc (dashed lines) Brillouin zones.

proach was first taken by Asano and Yamashita.⁶ At present, theoretically, the principal features of the PM and commensurate AF Cr band structures are well established.

Before showing the calculated AF band structure, it seems instructive to construct the band structure of commensurate AF Cr with a sc unit cell from the band structure of PM Cr with a bcc unit cell. The relationship between the sc and bcc Brillouin zones (BZ's) is shown in Fig. 1(b). We find that the ranges ΓN (Σ axis) and HN (G axis) coincide and G_1, G_2, G_3, G_4 have symmetry properties identical with $\Sigma_1, \Sigma_2, \Sigma_3, \Sigma_4$ for the sc case. As shown in Fig. 2, where the calculated energy bands for PM bcc Cr of Asano and Yamashita⁶ are plotted, the bands along the G axis (dashed lines) are folded back over those along the Σ axis (solid lines) as an approximation to the commensurate AF bands. The accidental degeneracy gives rise to the hybridization gap (AF energy gap), which is thought to stabilize the AF state. The most remarkable AF band gaps appear on the Λ axis and the Σ axis (schematically shown by dotted lines in Fig. 2) near the Fermi energy (E_F). Calculations assuming commensurate AF Cr show the AF gaps of typically 0.2 eV (Refs. 6 and 12) or 0.5 eV (Refs. 10 and 13). The existence of the AF gaps has been verified in an optical reflectance experiment,¹⁶ but not yet in an angle-resolved photoemission spectroscopy (ARPES) experiment. The AF energy

bands obtained by this folding procedure are found to be very much like the calculated ones of Refs. 6, 10, 12, and 13, except for the AF gaps.

On the experimental side, only a few ARPES investigations of the bulk band structure of Cr have been reported.^{1,2,4,5} Johansson *et al.*¹ measured normal-emission spectra of Cr(110) with photons from 15 to 31 eV to study the energy bands along the [110] (ΓM) direction and to observe the spectroscopic effects of the AF-PM magnetic-phase transition. However, good agreement with the AF bands of Asano and Yamashita⁶ was not obtained and no drastic temperature dependence was observed. Gewinner *et al.*² carried out off-normal ARPES experiments on Cr(100) using He I radiation to probe the energy bands along Γ - H - N - P . They found no evidence of the AF band properties. Klebanoff *et al.*⁴ investigated the surface and near-surface electronic structures of Cr(100) and presented photoemission evidence for a ferromagnetic phase transition in the surface layer, and for an AF phase in the near-surface region (see also Refs. 17 and 18). From their data, they concluded that a spectral feature unique to the near-surface AF phase disappeared by $\sim 3.3T_N$, in contrast to the behavior of electronic states present in both the AF and PM phases. To explain this, they thought that the presence of Cr(100) surface ferromagnetism produces a Cr(100) near-surface AF region with an enhanced magnetization. However, the results might better be reexamined in detail. Persson and Johansson⁵ used off-normal ARPES with He I and Ne I radiation to study the energy bands of Cr(110) along the [001] and $[\bar{1}10]$ directions, but they found no differences in the photoemission spectra recorded below and above T_N .

The purpose of this paper is to present the results of our recent normal-emission ARPES measurements of a clean Cr(110) surface at temperatures below and above T_N in the photon energy range of 20–120 eV. Particular emphasis is placed upon the investigations of the band structure of AF Cr along the [110] (ΓM) direction normal to the surface and the changes in the band structure caused by the magnetic-phase transition. Our results demonstrate that an emission from the Σ_3 band unique to the AF phase (corresponding to the G_3 band in the PM phase as shown in Fig. 2) disappears above T_N .

II. EXPERIMENT

The ARPES measurements using synchrotron radiation were conducted on Beam Line 11D of Photon Factory, National Laboratory for High Energy Physics, using a 150° spherical-sector-type electron-energy analyzer with an acceptance angle of $\pm 1^\circ$ as described elsewhere.^{19,20} Total experimental resolution was dependent on photon energy ($h\nu$); it varied smoothly from 0.1 eV for $h\nu=20$ eV to 0.6 eV for $h\nu=120$ eV, but was less than 0.2 eV for $h\nu < 60$ eV. Throughout the whole experiment, the surface component of the vector potential (\mathbf{A}) of the incident light was in the [001] azimuth (A_{\parallel} along [001]). Only photoelectrons emitted normally to the surface were collected. Data were normalized to the relative flux of incident photons. The working pressure of the instrument during the measurements was 1×10^{-10} Torr.

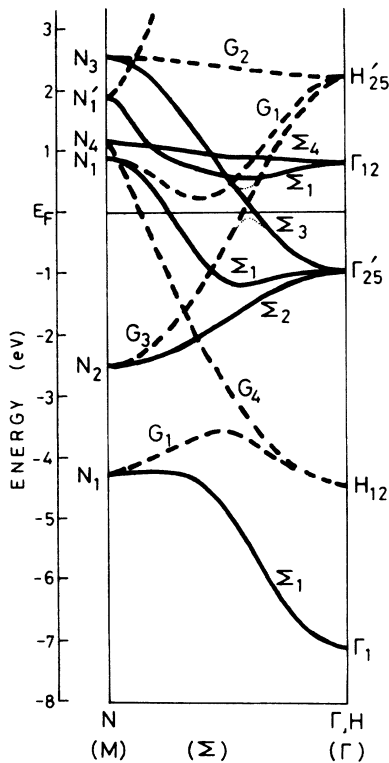


FIG. 2. Energy bands of PM bcc Cr along the [110] (ΓM) direction (solid lines) as calculated by Asano and Yamashita (Ref. 6). The PM bands from N to H (dashed lines) have been folded back over those from Γ to N as an approximation to the AF bands.

The Cr(110) single crystal which was oriented to within $\pm 0.5^\circ$ was the same one used in our previous experiments.²¹⁻²³ As reported previously, the sample was cleaned by repeated cycles of Ar⁺-ion sputtering (0.6–1.5 kV) and annealing (870–1150 K). The sample then displayed a very sharp, low-background (1×1) low-energy electron-diffraction (LEED) pattern. No impurities were detectable by Auger electron spectroscopy (estimated to be less than ~ 0.01 monolayer). Frequent flashing of the sample was made (~ 1150 K for a few minutes) in order to remove contamination of residual CO, and/or carbon and oxygen by decomposition of CO. The standard cleaning cycle (Ar⁺-ion sputtering and annealing) was repeated every 1–2 h, typically 1 h. The sample geometry was checked using LEED. With liquid-N₂ cooling, the sample could be cooled to ~ 80 K (within ~ 5 min from the annealing temperature of ~ 1150 K).

III. RESULTS AND DISCUSSION

Figure 3 shows normal-emission photoelectron spectra of the clean Cr(110) surface measured at 80 K (below T_N) and at a light incidence angle of $\theta_i = 25^\circ$ (predominant A_{\parallel} along [001] and small A_{\perp} along [110], parallel and normal to the surface) for $25 \leq h\nu \leq 80$ eV. The binding energy (E_b) is referred to E_F . The inset of this figure shows normal-emission spectra of Cr(110) taken at 80 K and $\theta_i = 60^\circ$ (both A_{\parallel} and A_{\perp}) for various $h\nu$. The prominent features between E_F and ~ 2 eV in these spectra are due to emission from the upper 3d bands as will be discussed later in detail. For $h\nu \geq 44$ eV, ordinary (incoherent) $M_{23}VV$ super Coster-Kronig (SCK) emission is observed as broad peaks marked by arrows at $E_b = h\nu - 37$ eV, i.e., at a fixed kinetic energy of $E_k = 37$ eV as referenced to E_F .²⁴ Two features marked by tic marks, around 3 and 6 eV below E_F , respectively, show small dispersion of 0.5–1 eV with $h\nu$ and are increased in intensity when increasing θ_i from 25° to 60° . These peaks are distinguishable from an emission, centered at ~ 6.2 eV, characteristic of the chemisorbed oxygen on Cr(110), which stays at the same location when $h\nu$ is changed.²⁵ For the normal-emission spectrum taken with A_{\parallel} along the [001] azimuth, in principle only initial states of Σ_1 and Σ_3 symmetry would be allowed according to symmetry selection rules for direct transition.²⁶ That is, an enhanced (reduced) emission from Σ_1 (Σ_3) initial states is expected when increasing θ_i from 25° to 60° . Therefore the two structures at ~ 3 and ~ 6 eV can be ascribed to the emission from the Σ_1 bulk bands.

The point to be stressed here is that, in contrast to the majority of the previous claims,^{1,2,27,28} we found no evidence for the existence of a valence-band satellite (two-bound-hole final state) in Cr in agreement with the results of Ref. 29. Reference 29 concluded the absence of a valence-band satellite in Cr based on the 3s core-level spectra reported therein, and the valence-band spectra for $h\nu = 16$ –24 and 90–120 eV (away from the 3p resonance region) in Refs. 4 and 18. As seen in Fig. 3, the main 3d-band emission intensity shows a resonant reduction at the 3p-3d excitation threshold of ~ 42 eV, but a

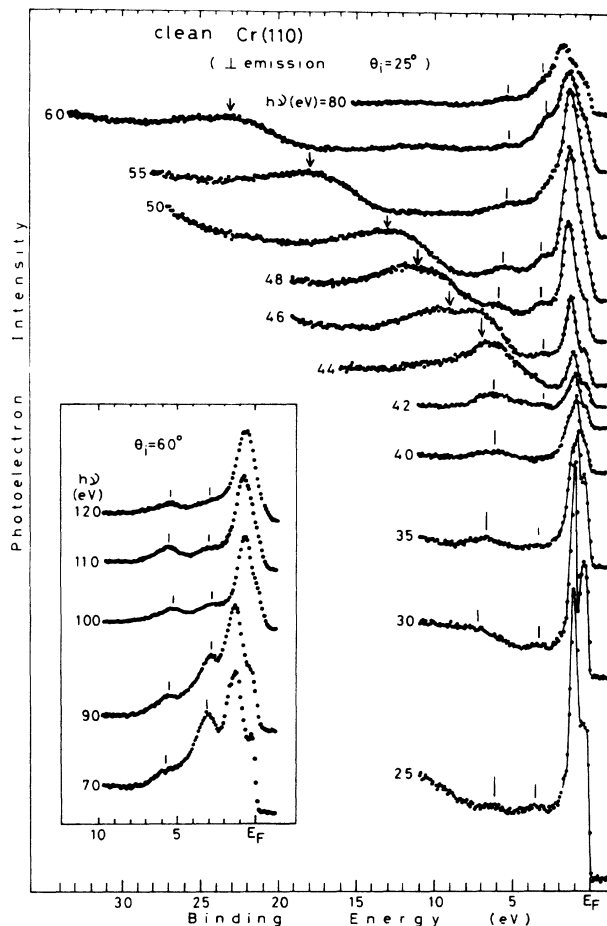


FIG. 3. Normal-emission spectra of clean Cr(110) measured at 80 K and $\theta_i = 25^\circ$ (A_{\parallel} along [001]) as a function of $h\nu$. The arrows indicate the expected position of the $M_{23}VV$ SCK line. The inset shows the $\theta_i = 60^\circ$ normal-emission spectra for various $h\nu$.

feature staying at a fixed binding energy around 6 eV (Refs. 1 and 28) or 7–7.3 eV (Refs. 2 and 27) is not found in the spectra measured for the clean Cr(110). Also, such a satellite would accompany 3p photoionization. Figure 4 shows the 3p core-level spectrum for Cr(110) measured

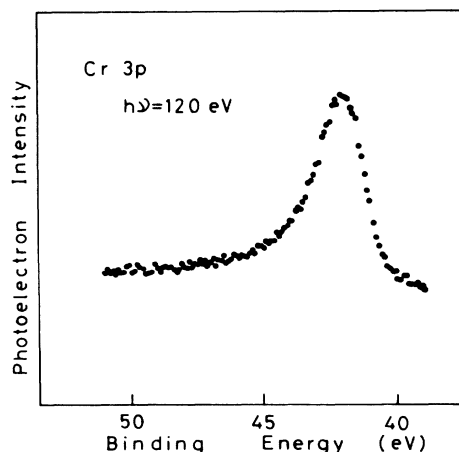


FIG. 4. Cr(110) 3p core-level spectrum measured at $h\nu = 120$ eV.

at $h\nu=120$ eV. We do not observe a satellite feature at 6–7 eV from the main 3*p* emission line with $E_b=42.0$ eV. We have demonstrated in the previous $h\nu$ -dependent ARPES experiments for clean Fe(110) (Ref. 19) and Ni(110) (Ref. 20) that a valence-band satellite exists in Ni, but not in Fe. The occurrence of the two-*d*-hole bound state does not appear to be realistic in transition metals with less than nine 3*d* electrons per atom (see Ref. 19).

The normal-emission spectra of Cr(110) in the low- E_b region between E_F and ~ 2 eV are shown in more detail in Fig. 5 ($\theta_i=60^\circ$) and Fig. 6 ($\theta_i=25^\circ$). These spectra were measured at 80 K. From detailed comparison with the $\theta_i=60^\circ$ and $\theta_i=25^\circ$ spectra, we find the Σ_3 -band

emission peak, which is marked by triangles in Fig. 6. If we assume primary-cone emission and a free-electron-like final-state band with Σ_1 symmetry and with an inner potential $V_0=9.8$ eV (Ref. 1) for the case of Cr(110), we can map the binding energies of all the observed peaks (e.g., Figs. 3, 5, and 6) onto points along the [110] (Γ - Σ - M) direction in the AF bulk BZ. All the experimental points plotted over the calculated bulk band structure of AF sc Cr by Asano and Yamashita^{6,30} along Γ - Σ - M are shown in Fig. 7 (circles except for the Σ_3 peak marked by crosses). With a few exceptions ($\sim 60 < h\nu < \sim 90$ eV and a peak at ~ 0.25 eV originating from a surface resonance, see below), each of the observed features has a theoretical

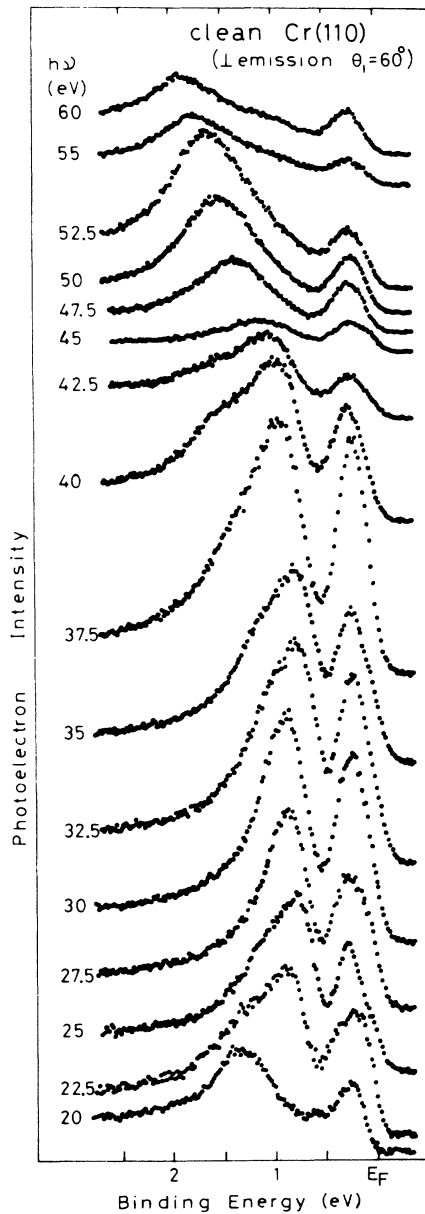


FIG. 5. Details of normal-emission spectra of clean Cr(110) for energies between E_F and ~ 2 eV, measured at 80 K and $\theta_i=60^\circ$ (A_{\parallel} along [001]) as a function of $h\nu$.

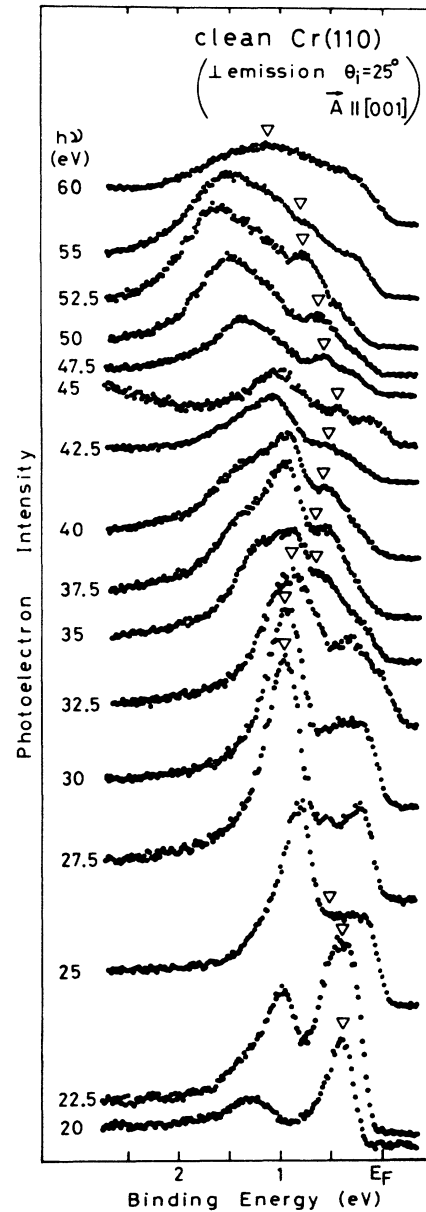


FIG. 6. As Fig. 5 but for $\theta_i=25^\circ$. Triangles indicate the position of the Σ_3 -band emission peak.

counterpart and the major trends in the experimentally determined dispersions are in most cases well reproduced by the calculated dispersions. For the upper bands between E_F and ~ 2 eV, the overall agreement between experimental and calculated results is good, though no emission should be observed from the Σ_2 band at normal emission. Johansson *et al.*¹ also observed the Σ_2 -band emission peaks in their normal-emission spectra of Cr(110). The possible explanation for this discrepancy will be described later. For the lower two Σ_1 bands, substantial discrepancies between measured and calculated dispersions exist. Firstly, the measured binding energies of the Σ_1 band originating from Γ_{12} are always lower than calculated. Similar results have been obtained by Johansson *et al.*¹ The binding energy of the critical point Γ_{12} is estimated to be ~ 3.4 eV, in agreement with the value reported by Gewinner *et al.*² Secondly, our data show that there exists a large gap (~ 2 eV) between M_1 and M_3 . On this point, the recent band calculations for AF Cr indicate that the degeneracies at the zone boundary are lifted and therefore the energy gaps appear at M , R , and X .^{10,13} However, the energy separation between M_1 and M_3 is calculated to be ~ 0.5 eV, which is considerably smaller than measured.

Let us consider possible explanations of the discrepancies between the experimental band structure and one-electron band calculations, i.e., observation of emission from the Σ_2 bulk band at normal emission and substantial disagreement between the measured and calculated bind-

ing energies for the lower Σ_1 bands.

(1) As suggested in Ref. 1, the acceptance angle of $\pm 1^\circ$ of the analyzer used may permit electrons excited from the Σ_2 band to be observed.

(2) For the range $\sim 60 < h\nu < \sim 90$ eV, the free-electron-like final-state band hypothesis may not be valid. That is, there may be no Bloch states of Σ_1 symmetry for ~ 60 – ~ 90 eV above E_F . Unfortunately, the band structure of Cr at energies higher than ~ 30 eV above E_F has not been calculated yet.

(3) The spin-orbit interaction (relativistic effect) which was neglected in the band-structure calculations might be important, since it mixes bands of different parity and gives rise to a gap.

(4) The difference between commensurate and incommensurate AF band dispersions may be responsible for such discrepancies, though it is believed to be small.⁴

(5) The final possible explanation is the deficiencies in the local approximation for exchange and correlation which the current band theory employs.

The physical origin of the observed discrepancies is not well understood at present and will hopefully be elucidated in future theoretical work.

Figure 5 shows the existence of a feature staying at a fixed binding energy of ~ 0.25 eV for various $h\nu$, indicating that this feature originates from a surface-induced state. This interpretation must be tested by studying its sensitivity to surface contamination. The typical effects observed are illustrated in Fig. 8, where the $\theta_i = 60^\circ$

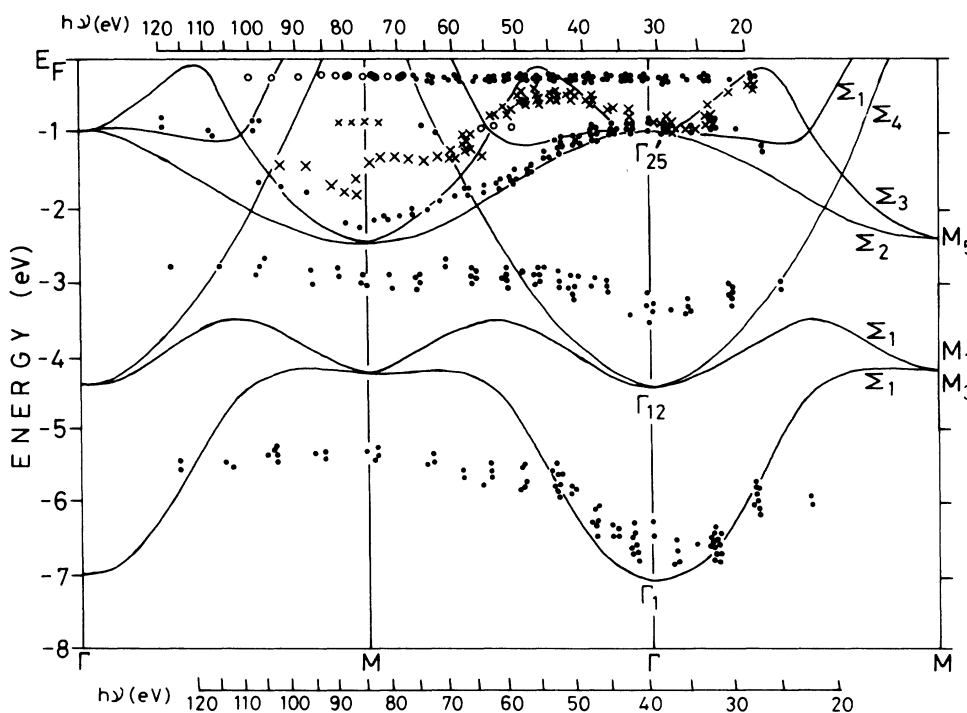


FIG. 7. Portions of the band structure of AF Cr along the [110] (ΓM) direction in the bulk BZ (the repeated-zone scheme). The binding energies of the peaks obtained by normal-emission measurements are represented by circles and crosses. The open circles and small crosses correspond to weak features. The solid curves denote the energy bands for the commensurate AF phase, calculated by Asano and Yamashita (Ref. 6).

normal-emission spectra of Cr(110) exposed to 1 L of oxygen [$h\nu=25$ eV, Fig. 8(a)] and to 20 L of hydrogen [$h\nu=30$ eV, Fig. 8(b)] are shown (1 L = 10^{-6} Torr sec). The feature at 0.25 eV is much affected by these exposures as compared with the feature located around 1 eV, originating from the bulk bands. A similar feature has been observed at 0.2–0.3 eV by Wincott *et al.*³ and Persson and Johansson.⁵ Since no absolute gap exists for $k_{\parallel}=0$ ($\bar{\Gamma}$), the observed feature at 0.25 eV in the normal-emission spectra is ascribed to the surface resonance. Our data indicate that this surface resonance possesses Σ_1 symmetry at $\bar{\Gamma}$, as suggested experimentally⁵ and theoretically.¹⁷ A weak shoulder is seen near E_F in the spectra of gas-covered surfaces (Fig. 8). This feature might be due to the truncation of a surface state by the Fermi level which is predicted to exist just above E_F .¹⁷

Finally, we show the observations of spectroscopic effects of AF to PM magnetic-phase transition. We measured the $\theta_i=25^\circ$ normal-emission spectra of Cr(110) at temperatures below and above T_N (i.e., 80 and 470 K) for various $h\nu$, as shown in Fig. 9. The positions of the Σ_3 -band emission peak observed in the $T=80$ -K spectra are indicated by triangles (see also Fig. 6). For $h\nu=40$ eV [Fig. 9(a)], no essential difference is observed in the spectra recorded at 80 K (below T_N) and 470 K (above T_N , $T=1.5T_N$). Similar results were obtained for $\sim 20 < h\nu < \sim 45$ eV. On the other hand, for $h\nu=52.5$

eV [Fig. 9(b)] and $h\nu=55$ eV [Fig. 9(c)], significant differences for the two different temperatures are observed in the feature corresponding to emission from the Σ_3 band. That is, the Σ_3 -band emission peak is observed below T_N (80 K), while this feature disappears above T_N (470 K). This phenomenon was found to be reversible. Such changes in the spectra cannot be explained by pure temperature broadening and smearing effects, since for Cr an increase in temperature from 80 to 470 K yields an energy broadening of only 0.006 eV (detailed discussion on the temperature effects was given in Ref. 1). Furthermore, according to Refs. 4 and 31, for Cr near T_N , the degree of BZ averaging due to phonon-assisted nondirect transitions could be only a few percent for $h\nu=40$ –100 eV. These findings seen in Fig. 9, i.e., the spectral changes does not occur for $h\nu=40$ eV but for $h\nu=52.5$ and 55 eV, can be understood in terms of the folded band structure of Fig. 2. As seen in Fig. 7, if assuming the free-electron-like final-state band with $V_0=9.8$ eV, the $h\nu=40$ -eV normal-emission spectrum probes the initial states for the k_{\perp} region between the Γ point and the point corresponding to the AF Σ_3 -band extreme (i.e., the point

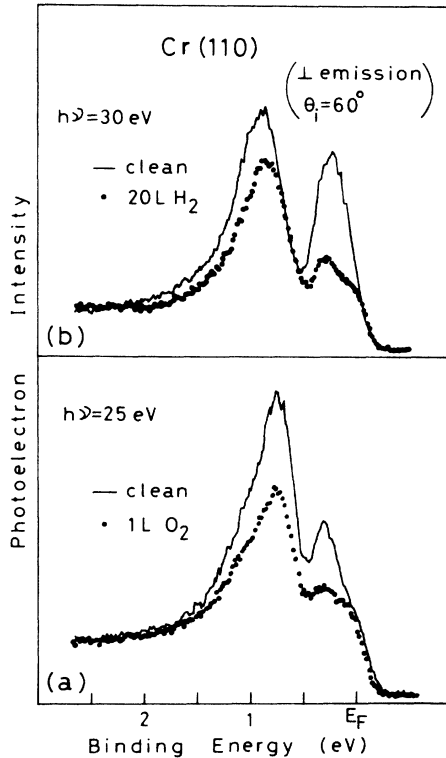


FIG. 8. (a) Normal-emission spectra of clean Cr(110) (line) and after exposure to 1 L of oxygen (dots), measured at $\theta_i=60^\circ$ and $h\nu=25$ eV. (b) Normal-emission spectra of clean Cr(110) (line) and after exposure to 20 L of hydrogen (dots), measured at $\theta_i=60^\circ$ and $h\nu=30$ eV.

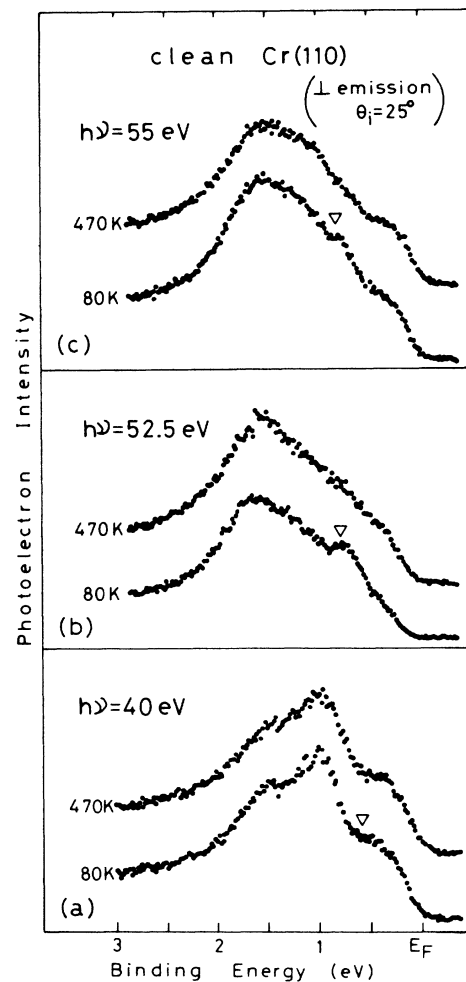


FIG. 9. Normal-emission spectra of clean Cr(110) measured at temperatures below and above T_N for (a) $h\nu=40$ eV, (b) $h\nu=52.5$ eV, and (c) $h\nu=55$ eV.

where the Σ_3 and G_3 bands cross in the folded band structure shown in Fig. 2). Figure 2 shows that for such a k_{\perp} region the Σ_3 band in the AF phase is essentially the same as the Σ_3 band in the PM phase, and therefore no significant spectral changes induced by the magnetic-phase transition can be expected. Thus, in this case ($\sim 20 < h\nu < \sim 45$ eV), the existence of the Σ_3 -band emission peak is possible for both the AF and PM phases. In contrast, for $h\nu = 52.5$ and 55 eV, the normal-emission spectra probe the initial states for the k_{\perp} region between the M point and the AF Σ_3 -band extreme point, where the Σ_3 band in the AF phase corresponds to the G_3 band along HN in the PM phase which should disappear in the PM band structure along ΓN . Therefore, for these photon energies, we can expect the disappearance of the Σ_3 -band emission peak above T_N . Thus, we consider that these results shown in Fig. 9 are spectroscopic observations of changes in the band structure caused by the *bulk* AF-PM magnetic-phase transition.

The ARPES work of Ref. 1 also reports a temperature-induced change in the Cr(110) Σ_3 band observed at -0.2 eV, and also assigns it to an AF-PM phase transition in Cr(110). However, the feature in question is still observed above T_N , though its intensity is somewhat reduced from that observed below T_N . Furthermore, according to our above discussion and Fig. 2 of Ref. 1, their normal-emission spectra recorded at $h\nu = 19$ and 21 eV probe the Σ_3 band essentially unique to the PM phase. Thus, their observation has very little to do with the AF-PM phase transition.

IV. CONCLUSION

Most of the features observed in the $h\nu$ -dependent normal-emission spectra of the Cr(110) surface can be in-

terpreted in terms of direct transitions from bulk bands to a free-electron final band, though there exist some discrepancies between experiment and band theory which are poorly understood at present. A surface resonance with $E_b = 0.25$ eV at $\bar{\Gamma}$ ($k_{\parallel} = 0$) is found for clean Cr(110). In contrast to the case of Cr(100),⁴ a Cr(110) surface is expected to be AF since the simple AF bcc structure demands that the (110) plane contains an equal number of up and down spins. Our data are consistent with the near-surface AF periodicity *normal* to the surface.

The temperature dependence of the AF Σ_3 -band emission intensity was investigated and prominent effects on the *bulk* band structure caused by the AF-PM magnetic-phase transition have been observed near T_N . The present work clearly demonstrates this phenomenon in Cr by means of ARPES.

Note that we found no evidence for a valence-band satellite in Cr. From this result and our previous ARPES data for Fe(110) (Ref. 19) and Ni(110) (Ref. 20), we can say that the occurrence of a multielectron valence-band satellite does not appear to be realistic in transition metals with less than nine 3d electrons per atom.

ACKNOWLEDGMENTS

We are pleased to thank the staff of Photon Factory, National Laboratory for High Energy Physics, particularly T. Miyahara, for their excellent support. This work has been performed under the approval of the Photon Factory Program Advisory Committee (Proposal No. 86-150).

- ¹L. I. Johansson, L. G. Petersson, K. F. Berggren, and J. W. Allen, *Phys. Rev. B* **22**, 3294 (1980).
²G. Gewinner, J. C. Peruchetti, A. Jaéglé, and R. Pinchaux, *Phys. Rev. B* **27**, 3358 (1983).
³P. L. Wincott, N. B. Brookes, D. S. Law, G. Thornton, and H. A. Padmore, *Vacuum* **33**, 815 (1983).
⁴L. E. Klebanoff, S. W. Robey, G. Liu, and D. A. Shirley, *Phys. Rev. B* **30**, 1048 (1984); **31**, 6379 (1985).
⁵P. E. S. Persson and L. I. Johansson, *Phys. Rev. B* **33**, 8814 (1986); **34**, 2284 (1986).
⁶S. Asano and J. Yamashita, *J. Phys. Soc. Jpn.* **23**, 714 (1967).
⁷J. Rath and J. Callaway, *Phys. Rev. B* **8**, 5398 (1973).
⁸K. H. Oh, B. N. Hermon, S. H. Liu, and S. K. Sinha, *Phys. Rev. B* **14**, 1283 (1976).
⁹J. L. Fry, N. E. Brener, J. L. Thompson, and P. H. Dickinson, *Phys. Rev. B* **21**, 384 (1980).
¹⁰J. Kübler, *J. Magn. Magn. Mater.* **20**, 277 (1980).
¹¹D. G. Laurent, J. Callaway, J. L. Fry, and N. E. Brener, *Phys. Rev. B* **23**, 4977 (1981).
¹²H. L. Skriver, *J. Phys. F* **11**, 97 (1981).
¹³N. I. Kulikov and E. T. Kulatov, *J. Phys. F* **12**, 2291 (1982).
¹⁴A. W. Overhauser, *Phys. Rev.* **128**, 1437 (1962).
¹⁵W. M. Lomer, *Proc. Phys. Soc. London* **80**, 489 (1962); **84**, 327 (1964).
¹⁶A. S. Barker, Jr., B. I. Halperin, and T. M. Rice, *Phys. Rev.*

Lett. **20**, 384 (1968).

- ¹⁷R. H. Victora and L. M. Falicov, *Phys. Rev. B* **31**, 7335 (1985).
¹⁸L. E. Klebanoff, R. H. Victora, L. M. Falicov, and D. A. Shirley, *Phys. Rev. B* **32**, 1997 (1985).
¹⁹H. Kato, T. Ishii, S. Masuda, Y. Harada, T. Miyano, T. Komeda, M. Onchi, and Y. Sakisaka, *Phys. Rev. B* **32**, 1992 (1985); **34**, 8973 (1986).
²⁰Y. Sakisaka, T. Komeda, M. Onchi, H. Kato, S. Masuda, and K. Yagi, *Phys. Rev. Lett.* **58**, 733 (1987); *Phys. Rev. B* **36**, 6383 (1987).
²¹H. Kato, Y. Sakisaka, M. Nishijima, and M. Onchi, *Surf. Sci.* **107**, 20 (1981).
²²H. Kato, Y. Sakisaka, T. Miyano, K. Kamei, M. Nishijima, and M. Onchi, *Surf. Sci.* **114**, 96 (1982).
²³Y. Sakisaka, H. Kato, and M. Onchi, *Surf. Sci.* **120**, 150 (1982).
²⁴The SCK emission seems to contain at least two contributions with $E_k = 36$ and 38 eV which have different weights depending on $h\nu$.
²⁵T. Komeda, Y. Sakisaka, M. Onchi, H. Kato, S. Suzuki, K. Edamoto, and Y. Aiura (unpublished).
²⁶J. Hermanson, *Solid State Commun.* **22**, 9 (1979).
²⁷D. Chandesris, J. Lecante, and Y. Petroff, *Phys. Rev. B* **27**, 2630 (1983); **34**, 8971 (1986).

²⁸H. Sugawara, K. Naito, T. Miya, A. Kakizaki, I. Nagakura, and T. Ishii, *J. Phys. Soc. Jpn.* **53**, 279 (1984).

²⁹L. E. Klebanoff and D. A. Shirley, *Phys. Rev. B* **33**, 5301 (1986).

³⁰Although the Korringa-Kohn-Rostoker band calculations of AF and PM Cr by Asano and Yamashita (Ref. 6) were made by using a special fitting scheme in order to obtain the average spin densities and therefore their calculations were not

completely self-consistent, their results are rather similar to the recent ones obtained by modern computational techniques (Refs. 7–13) and have most frequently been referred in the literature as the standard of band calculation of Cr.

³¹R. C. White, C. S. Fadley, M. Sagurton, P. Roubin, D. Chandris, J. Lecante, C. Guillot, and Z. Hussain, *Solid State Commun.* **59**, 633 (1986); *Phys. Rev. B* **35**, 1147 (1987).